Highlights of Spanish Astrophysics XI, Proceedings of the XV Scientific Meeting of the Spanish Astronomical Society held on September 4–9, 2022, in La Laguna, Spain. M. Manteiga, L. Bellot, P. Benavidez, A. de Lorenzo-Cáceres, M. A. Fuente, M. J. Martínez, M. Vázquez- Acosta, C. Dafonte (eds.), 2023

Stellar Populations in type Ia supernova host galaxies at intermediate-high redshift: Star formation and metallicity enrichment histories.

Millán-Irigoyen, I.[1], del Valle-Espinosa, M. G.[2], Fernández-Aranda, R.[3], Galbany, L.[4,5], Gomes, J.M.[6], and Mollá, M.[1]

[1] Dpto. de Investigación Básica, CIEMAT, Avda. Complutense 40, E-28040 Madrid, Spain
[2] Institute for Astronomy, The University of Edinburgh, Royal Observatory, Blackford Hill, Edinburgh, EH9 3HJ, UK
[3] Institute of Astrophysics - FORTH & Dept. of Physics ,University of Crete, 70 013 Heraklion, Greece
[4] Institute of Space Sciences (ICE, CSIC), Campus UAB, Carrer de Can Magrans, s/n, E-08193 Barcelona, Spain
[5] Institut d'Estudis Espacials de Catalunya (IEEC), E-08034 Barcelona, Spain
[6] Instituto de Astrofísica e Ciências do Espaço, Universidade do Porto, CAUP, Rua das Estrelas, 4150-762 Porto, Portugal

Abstract

We describe our project to study galaxies hosting type Ia supernova (SN Ia) at different redshifts. We present optical spectroscopy of 6 galaxies at redshift $z \sim 0.45$ observed with Gran Telescopio de Canarias. They are joined to a set of SN Ia host galaxies at intermediate-high redshift, taken from SDSS and COSMOS surveys. After some selection cuts, in terms of signal-to-noise and other criteria, our final sample consists of 680 galaxies in the range $0.04 < z < 1$ of redshift. We perform an inverse stellar population synthesis with the code FADO to estimate the star formation histories. We simultaneously obtain their stellar mass, and their mean stellar age and metallicity. We then look for possible correlations of the Hubble diagram residuals and of the supernova light curve features (luminosity, color and strength) on these stellar parameters. We find that the Hubble diagram residuals show a correlation with the weighted by mass stellar metallicity (in logarithmic scale) with a slope of -0.061 $\mathrm{mag\,dex^{-1}}$. This result supports our previous findings obtained with gas oxygen abundances for local and SDSS galaxies. This is also similar to the value found in other works from the literature. Our result is in agreement with others, but it is obtained with more precision and a better significance due to the higher number of objects and wider range of redshift of our sample.

1 Introduction

Type Ia supernova (SN Ia) have been used as standard candles from the mid 1990s to measure the evolution of the Universe with sufficient precision and at distances large enough to detect an accelerated rate of expansion of the Universe, in the High-z Supernova project [25] and the Supernova Cosmology Project [22].

The SN Ia brightness can be standardized, to use their light-curves and their apparent peak magnitude (m) to estimate distances to their host galaxies. Assuming an universal absolute peak magnitude (M), their distance modulus ($\mu = m - M$) can be represented as a function of the redshift (z) of their host galaxy, in the well known Hubble diagram (HD). However, SNe Ia are not natural standard candles but *standardizable* by means of a relationship between their peak brightness m, and the width of their light-curves (parametrized by $x1$, s, or Δm_{15}), and their color (c or $E(B-V)$) at the peak [23, 24, 32].

This standardization technique is mainly trained with SNe Ia of galaxies of the Local Universe, with typically around Solar abundances and stellar ages. In fact, there are theoretical models that predict that the metallicity of the progenitor system would affects the luminosity of the SN Ia: [30] showed that the excess of neutrons in the explosion of a white dwarf is a direct function of the metallicity of the progenitor star, and that this excess is what controls the ratio between radioactive (as ^{56}Ni, which defines the brightness of the explosion) to non-radioactive (elements of the group of iron) abundances.

There have been a large number of works for the last two decades studying possible correlations between parameters of the SN Ia and the characteristics of the explosion [7, 12, 21] The majority of them showed that SN Ia in massive host galaxies are brighter than less massive ones, after LC shape and color corrections. Considering the mass-metallicity relation [8], it migth to indicate a correlation between the magnitudes of SNe Ia and the metallicity of their host galaxies: the most metallic galaxies would have the brightest SNe Ia with a difference of $\sim 0.10\,\mathrm{mag\,dex^{-1}}$ with the less metallic ones.

The direct dependence of SNe Ia luminosities on metallicity was early studied by [6] and [7], who estimated the oxygen abundance using emission lines in star-forming galaxies, and the absorption stellar features in early-type galaxies respectively. In both cases, they found a trend between magnitudes of SNe Ia and the stellar population metallicity of their host galaxies.

We started a project to compute the possible effect of the metallicity of each SNe Ia in its brightness. For that we try to estimate the stellar metallicity of their hosting galaxies or the Oxygen abundance of their interstellar medium, to look for possible correlations between the SNe Ia brightness and those estimates of metallicity, trying to have a redshift range as wide as possible and a number of objects as high as possible. This is the final step of the project [17, 18, 19]. We reanalyse the previous works at intermediate redshift and extend it to higher redshift, up to $z \approx 1$.

First, we present the sample and the selection criteria in Section 2. Then, in Section 3 we present the analysis code FADO [10] that we use to obtain information of the stellar populations. Our results are presented in Section 4. Our conclusions are given in Section 5.

2 Observational data

We compiled spectra of SN Ia host galaxies from 3 different sources focusing on different redshift ranges.

- The low-intermediate redshift SN Ia sample is provided by the SDSS-II/SNe in their Data Release [26]. It is made of 1066 SNe Ia confirmed either spectroscopically (352 spec-Ia) or photometrically, identified based on a Bayesian LC fitting, using the spectroscopic redshift of their host galaxy (714 photo-Ia, [26]), and with publicly available host galaxy spectra in the 16th data release of the SDSS [1]. The sample is similar to the one presented in [19] and [5], where we have now performed aperture corrections to several host galaxy parameters.

- The intermediate redshift sample is made of 6 selected galaxies from the sample Union2.1 [29] at redshift $z \approx 0.45$ that were observed with GTC/OSIRIS [4] in long-slit mode, between November 2014 and January 2015 under the GTC57-14B programme (PI:Moreno-Raya). We set the width of the slit to 0.8 arcsec and used the R1000R grating, which provides spectral coverage in the range from 5100 to 10000 Å, with a resolving power of $R \sim 1100$.

  The data were reduced using the standard packages available for the bias subtraction, flat field correction and cosmic ray rejection and wavelength and flux calibration using the same procedure as in [18] from IRAF software [31]. Moreover, we have corrected the spectra for extinction effect, using the DEREDDEN task together with the tabulated values for the galactic extinction map available in [27].

- The high-z sample of SNe Ia ($0.5 \leq z \leq 1.0$) was taken from the Supernova Legacy Survey[1] (SNLS, [11, 2]). SNLS targeted four regions of $1° \times 1°$ in the sky, named from D1 to D4. The SNLS D2 region overlapped with the COSMOS extragalactic survey [28] footprint[2]. COSMOS consisted of a multi-wavelength imaging and spectroscopy of a region of the sky of $2° \times 2°$ centered at the J2000 coordinates (RA,Dec)=(+150.1191, +2.2058), using a multitude of telescopes. In particular, for our study we took spectra from the COSMOS sub-surveys *Magellan* [33] and *zCOSMOS*, [14].

  We crossmatched the coordinates of SN and the galaxy, with a selection criteria (i) a physical projected distance of 50 kpc between the SN position and the center of the galaxy, and (ii) a redshift relative error of 10%. We found that 44 matches (39 from zCOSMOS and 5 from Magellan) that meet both criteria, 3 of them being galaxies repeated in both surveys. We made a visual inspection with Hubble Space Telescope (HST) I-band images to make sure that the galaxy was the real host of the SN. A total of 28 galaxy-SN pairs was finally considered for further analysis.

The complete sample consists of 1087 galaxies (1053 from SDSS, 6 from GTC-OSIRIS and 28 from COSMOS) with available spectra. From them, we keep 803 galaxies (769 from

[1] https://www.cadc-ccda.hia-iha.nrc-cnrc.gc.ca/en/cfht/cfhtls.html
[2] https://irsa.ipac.caltech.edu/data/COSMOS/tables/spectra/

SDSS, 6 from GTC and 28 from COSMOS) that have spectra with $S/N > 3$. Additionally, we perform some cuts based on the SN Ia light-curve properties: the light-curve stretch in the range $-3 < x1 < 3$ and color in the range $-0.3 < c < 0.3$. We choose these ranges of $x1$ and c to match the training data of the SALT2 [11] empirical SNe Ia model, that was trained in those ranges of stretch and color. The final sample consists in 680 galaxies: 654 from SDSS, 6 from GTC and 20 from COSMOS, for which we have the complete information necessary for our analysis.

3 Analysis

Once selected the spectra of the 680 galaxies[3], we proceed to their analysis using the code FADO [10]. Fado tries to find the best fitting combination of stellar spectra using a basis of Simple Stellar Populations (SSPs). SSPs are sets of stars of the same age and metallicity whose spectra are calculated as the sum of spectra of individual stars that form them. In this work we use as *basis* the set of SSP calculated with the HR-PopStar code from [15]. For this work, we have developed a special set of models, that uses the spectral library of normal from [20], which has a shorter wavelength range than the original HR-pyPopStar, from 2500 Å to 10000 Å, but a wider range in metallicities, $0.0001 < Z < 0.05$.

Since we are working with non-local galaxies, it is necessary to take into account the age of the Universe in each redshift. These galaxies could not have stellar populations older than that age of the Universe corresponding to their redshift. Thus, the stellar populations older than this value can not exist nor contribute to the spectra.

4 Results

First, we have looked for two classical relations between the characteristics of the galaxy: mass-metallicity and age-mass relation. Concerning mass-metallicity relation, we find a similar relation than [8] and [9]. We have a similar relation to both authors, but with more dispersion, because we find a larger number of galaxies with low metallicity than them. In the case of age-mass relation, shown in Fig. 1a, we find younger stellar populations than [8]. We suggest that this difference is caused by the difference in the SSP basis used in the analysis, because the SSPs used in both works are different, HR-pyPopStar being specially tuned for the young SSPs models.

Then, we have computed the Hubble diagram of the SN using the calibration of [26] and the Hubble residuals (HR) using the cosmological distance modulus from the cosmological parameters from the same work, using a standard flat Λ CDM cosmology. From the whole sample of 680 galaxies, we have selected 664 for which $|HR| < 1.0$ mag to analyse the HR results and their dependence on the logarithm of stellar metallicity and current mass. We find correlations in both cases with slopes -0.061 mag dex^{-1} and -0.06 mag dex^{-1}, respectively. We show in Fig. 1b) the correlation of HR with the mean stellar metallicity in logarithmic

[3]The used spectra are in https://github.com/HOSTFLOWS

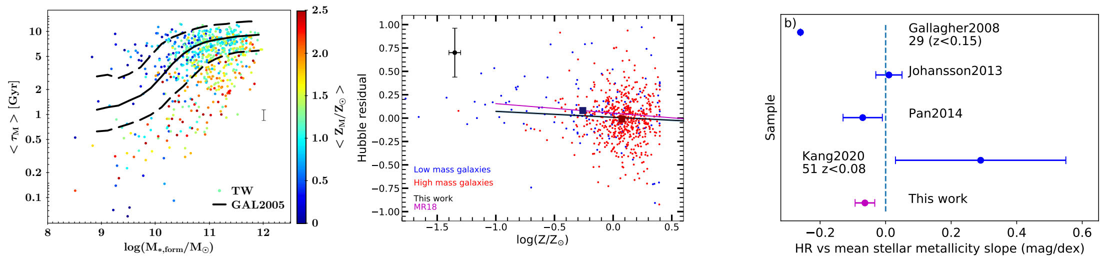

Figure 1: a) Stellar Mass-Age relation compared with [8] results; b) Hubble residuals *vs* the logarithm of the mean stellar metallicity weighted by mass, with the correlation found, the comparison with [19] and the blue and red squares that represent the mean HR of the low mass and the high mass bins respectively; and c) comparison of our results with the ones from [7, 12, 21, 13].

scale.

Finally, we have compared with other work of the literature that have measured the mean metallicity of the stellar population [7, 12, 21, 13] in Fig. 1c). Our results are similar to [21], but with smaller error and with the highest significance of all the works.

5 Conclusions

We have done a study of hosting SN Ia galaxies spectra for a redshift range of $0.1 < z < 1.0$. After analyzing with the FADO code, we have estimated the SFHs, $\langle Z_M \rangle$, $\langle Z_L \rangle$, $\langle \tau_M \rangle$, $\langle \tau_L \rangle$, v_{sys}, σ_{star}, M_{formed} and M_{present}. We present our results in [16] where more details may be found.

The two most important conclusions we find are: 1) The HR-pyPopStar models give younger stellar populations when using with FADO compared with previous models; and 2) The residuals of the Hubble diagram, HR, shows a clear dependence with the stellar metallicity, weigthed by mass, when is represented in logarithmic scale, with a slope of -0.059 mag dex^{-1}. This results is similar to others from the literature [7, 12, 21, 13] but we have the highest significance compared with all of them.

Acknowledgments

Based on observations made with the Gran Telescopio Canarias (GTC), installed at the Spanish Observatorio del Roque de los Muchachos of the Instituto de Astrofísica de Canarias, in the island of La Palma.

This research has made use of the HST-COSMOS database, operated at CeSAM/LAM, Marseille, France.

References

[1] Ahumada R., Prieto C. A., Almeida A., et al., 2020, ApJS, 249, 3.

[2] Betoule M., Kessler R., Guy J., Mosher J., et al., 2014, A&A, 568, A22.

[3] Bruzual G., Charlot S., 2003, MNRAS, 344, 1000.

[4] Cepa J., 2010, ASSP, 14, 15.

[5] Galbany L., Smith M., Duarte Puertas S., et al., 2022, A&A, 659, A89.

[6] Gallagher J. S., Garnavich P. M., Berlind P., et al., 2005, ApJ, 634, 210.

[7] Gallagher J. S., Garnavich P. M., Caldwell N., et al., 2008, ApJ, 685, 752.

[8] Gallazzi A., Charlot S., Brinchmann J., White S. D. M., Tremonti C. A., 2005, MNRAS, 362, 4

[9] González Delgado R. M., Cid Fernandes R., García-Benito R., et al., 2014, ApJL, 791, L16.

[10] Gomes J. M., Papaderos P., 2017, A&A, 603, A63.

[11] Guy J., Sullivan M., Conley A., et al., 2010, A&A, 523, A7.

[12] Johansson J., Thomas D., Pforr J., et al., 2013, MNRAS, 435, 1680.

[13] Kang Y., Lee Y.-W., Kim Y.-L., Chung C., Ree C. H., 2020, ApJ, 889, 8.

[14] Lilly S. J., Le Fèvre O., Renzini A., et al., 2007, ApJS, 172, 70.

[15] Millán-Irigoyen I., Mollá M., Cerviño M., et al., 2021, MNRAS, 506, 4781.

[16] Millán-Irigoyen, I., del Valle-Espinosa, M. G., Fernández-Aranda, R., et al. 2022, MNRAS, 517, 3312.

[17] Moreno-Raya M. E., Mollá M., López-Sánchez Á. R., Galbany L., et al., 2016, ApJL, 818, L19.

[18] Moreno-Raya M. E., López-Sánchez Á. R., Mollá M., et al., 2016, MNRAS, 462, 1281.

[19] Moreno-Raya M. E., Galbany L., López-Sánchez Á. R., et al., 2018, MNRAS, 476, 307.

[20] Munari U., Sordo R., Castelli F., Zwitter T., 2005, A&A, 442, 1127.

[21] Pan Y.-C., Sullivan M., Maguire K., et al., 2014, MNRAS, 438, 1391.

[22] Perlmutter S., Aldering G., Goldhaber G., et al., 1999, ApJ, 517, 565.

[23] Phillips M. M., 1993, ApJL, 413, L105.

[24] Riess A. G., Press W. H., Kirshner R. P., 1996, ApJ, 473, 88.

[25] Riess A. G., Filippenko A. V., Challis P., et al., 1998, AJ, 116, 1009.

[26] Sako M., Bassett B., Becker A. C., et al., 2018, PASP, 130, 064002.

[27] Schlegel D. J., Finkbeiner D. P., Davis M., 1998, ApJ, 500, 525.

[28] Scoville N., Aussel H., Brusa M., et al., 2007, ApJS, 172, 1.

[29] Suzuki N., Rubin D., Lidman C., et al., 2012, ApJ, 746, 85.

[30] Timmes F. X., Brown E. F., Truran J. W., 2003, ApJL, 590, L83.

[31] Tody D., 1993, ASPC, 52, 173

[32] Tripp R., 1998, A&A, 331, 815

[33] Trump J. R., Impey C. D., Elvis M., et al., 2009, ApJ, 696, 1195.